Supplement of Atmos. Meas. Tech., 11, 3491–3509, 2018
https://doi.org/10.5194/amt-11-3491-2018-supplement

Atmospheric Measurement Techniques
Open Access
EGU

Supplement of

Fast time response measurements of particle size distributions in the 3–60 nm size range with the nucleation mode aerosol size spectrometer

Christina Williamson et al.

Correspondence to: Christina Williamson (christina.williamson@noaa.gov)

Supplementary Material

S1. NMASS CPC dimensions

Table S1: Key dimensions of the NMASS CPC unit

Component	Length (mm)	Inner Diameter (mm)	Outer Diameter (mm)
Sample inlet	31.6	11.0	15.9
Saturator (post capillary)	22.9	14.8	31.8
Condenser	59.5	13.4	31.8
Optics nozzle	24.1	18.9	34.2
Aerosol Injector Tube 1	49.2	3.8	3.0
Aerosol Injector Tube 2	43.0	6.0	7.0
Capillary tube	19.1	0.83	1.07

S2. Kelvin Diameter Calculations

The saturation vapour pressure at the saturator and condenser temperatures (T_{sat} and T_{cond}) is given either by Eq. S1 in the case of diethylene-glycol and Fluorinert, or Eq. S2 in the case of n-butanol, where T in both cases is the temperature in Kelvin:

$$log_{10}P_s = a - \frac{b}{T-c} \quad \text{(S1)}$$

$$log_{10}P_s = \frac{-52.3b}{T} + c, \quad \text{(S2)}$$

where a, b, and c are empirical coefficients (Table S2). Following Baron and Willeke (2001), the surface tension, γ, and molar volume, ν, (Table S1) are used to relate the saturation vapour pressure on a droplet surface to D^*, as given by Eq. S3 (Hinds, 1999):

$$D^* = \frac{4v\gamma}{RTln\left(\frac{P_S(T_{sat})}{P_S(T_{cond})}\right)}. \quad \text{(S3)}$$

Table S2. Material properties of n-butanol, diethylene glycol and Fluorinert FC-43 for calculating the Kelvin diameter.

	Surface Tension mN m^{-1} at 25°C	Molar Mass g mol^{-1}	Mass Density g cm^{-3} at 20-25 °C	a	b	c
Butanol	24.2[1]	74.12[1]	0.81[2]	-	46.78[3]	11.26[3]
Diethylene-Glycol	55.1[5]	106.12[4]	1.114[5]	7.7007954[6]	2019.25[6]	-99.494[6]
Fluorinert, FC-45	16[7]	670[8]	1.860[8]	10.511[8]	2453[8]	0[8]

[1]The Dow Chemical Company (2012), [2]National Center for Biotechnology Information, [3]Baron and Willeke (2001), [4]Macdonald and Lide (2003), [5]Yaws (2008), [6]MEGlobal (2005), [7]3M Electronics (2009), [8]3M Performance Materials (2000).

S3. Orifice Changer for Pressure Control System

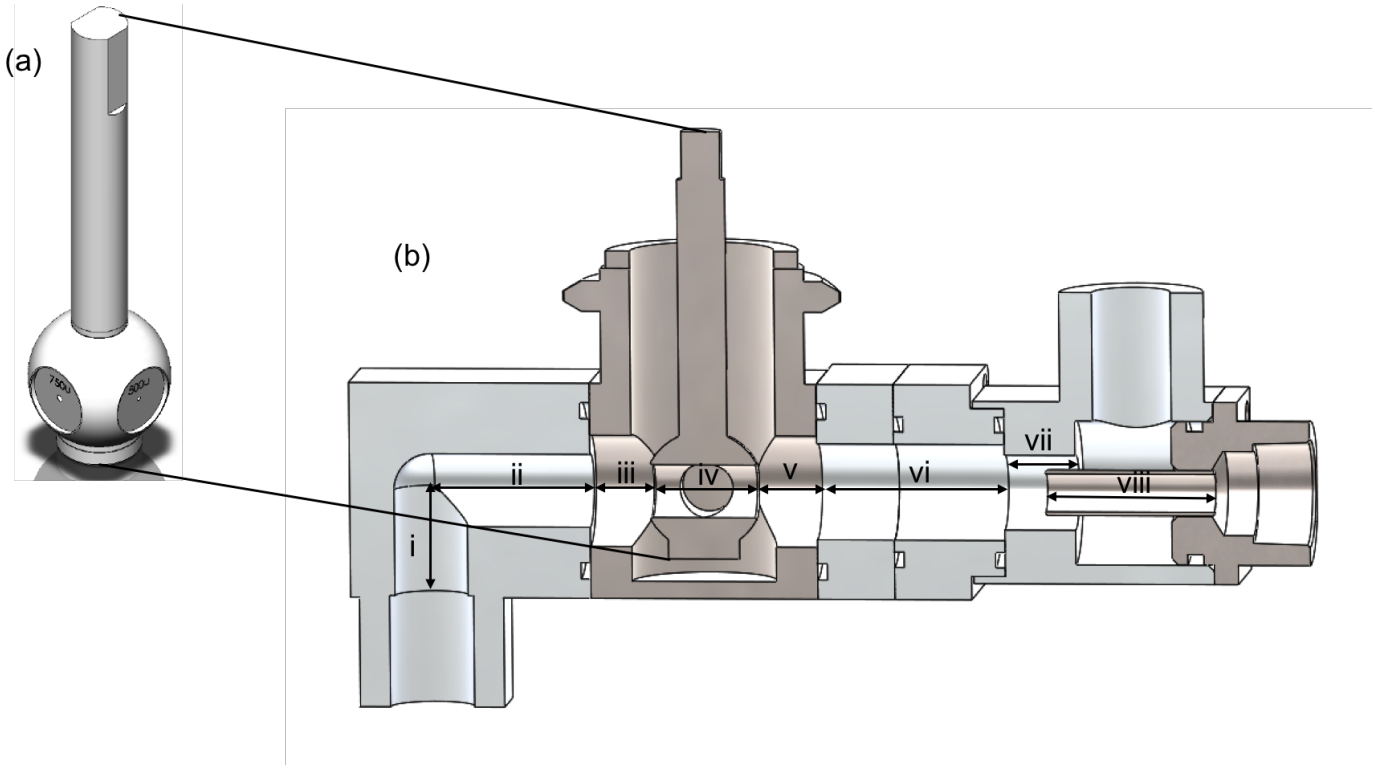

Fig. S1 Schematic of the orifice changer system used to keep internal pressure of the NMASS at 120 hPa while ambient pressure varies between 200 and 1034 hPa. Two orifices are brazed onto a drilled-out ball valve (a), which is turned by an actuator to select an orifice depending on the upstream pressure. The components of a pressure reducing inlet system (b) based on the University of Minnesota design (Lee et al., 1993) are attached to the valve-and-orifice system. Air enters the assembly from the bottom left, and the sample flow exits via a centerline extractor (viii) to the CPCs with minimised particle losses. Excess flow exits top right and is used to maintain the pressure and flow rate within the NMASS. Key dimensions are given in table S3.

Table S3. Key dimensions of the orifice changer for pressure control system

Part	Length (mm)	Inner Diameter (mm)
i	14.0	9.7
ii	21.1	9.7
iii	8.3	14.7
iv*	30.0	9.7
v	8.3	14.7
vi	24.8	12.7
vii	9.4	9.9
viii	22.2	5.0

*dimensions of the path of the flow through the ball valve

S4. Nano-DMA sizing uncertainties

Table S4. Nano-DMA parameters and uncertainties used to calculate calibration diameter uncertainties for the NMASS calibrations.

Parameter	Mean	Uncertainty
Sheath Flow (lpm)	5.1	0.1
Aerosol Pressure (hPa)	917	1
DMA voltage (V)	200	0.5%
DMA column outer diameter (m)	0.03613	2.54e-5
DMA column inner diameter (m)	0.0312	2.54e-5
DMA column length (m)	0.34054	2.54e-5

S5. Monte Carlo simulations

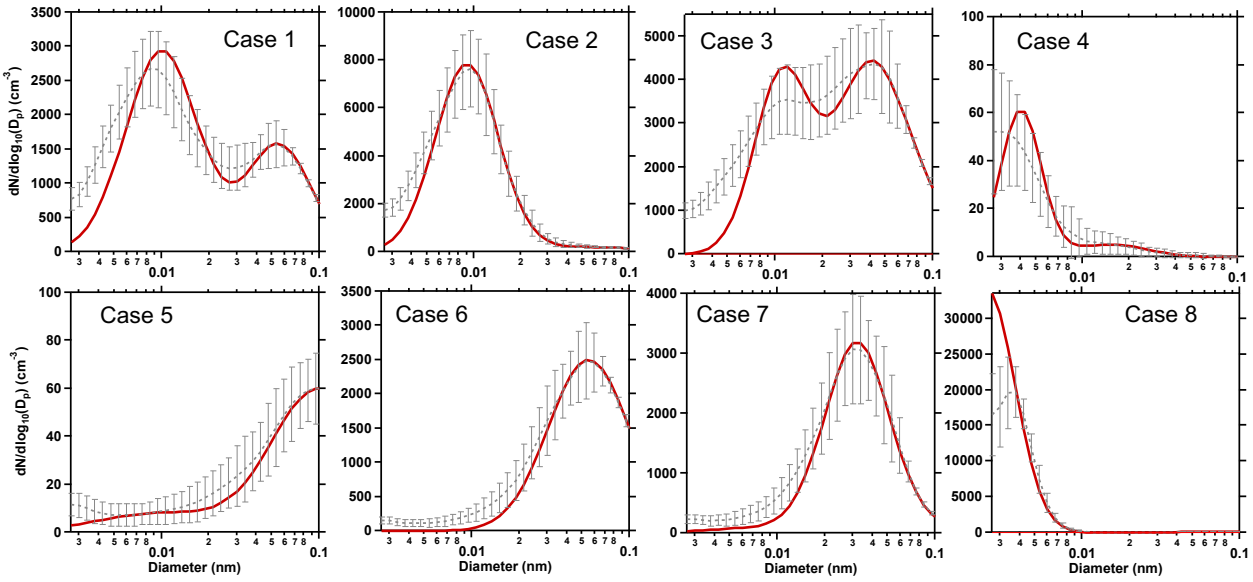

Fig. S2 Lognormal size distributions described by parameters in Table 2 of main text (solid red line), and mean and standard deviation from 1000 Monte Carlo simulations of inversion of instrument response calculated from the lognormal size distribution. Noise was added to each of the simulated instrument responses (CPC concentrations) to represent counting and concentration uncertainties. The instrument response curves (Fig. 5 in the main text) were also independently shifted in diameter by an amount equal to the observed variation during multiple calibrations.

S6. Verification of custom-built DMA and nano-SMPS performance

A custom-built DMA was used to generate the calibration aerosol used for comparison between a nano-SMPS and the NMASS in Fig. 10. The performance of this DMA was verified by atomizing a nearly monodisperse polystyrene latex (PSL) sphere aerosol with a peak diameter of 152 ± 5 nm and a polydispersity of 2.1% (ThermoFisher Scientific Series 3000 nanospheres). A CPC measured the concentration of particles exiting the DMA as the voltage was manually stepped across the peak in the transmission function (Fig. S3). A fitted Gaussian curve gives a peak diameter of 151.3 nm and a full-width at half-max (FWHM) of 17.4 nm (11.4%). The fitted peak diameter agree with the PSL size standards within uncertainties. The FWHM of the distribution is very close to the expected FWHM of 16.9 nm (11.1%) calculated from DMA theory (Knutson and Whitby, 1975) with the 10:1 sheath/aerosol flow ratio used and accounting for the polydispersity of the PSL. Thus the custom-built DMA is working close to theoretically optimal performance.

The custom-built DMA was used to produce a size-classified, atomized ammonium sulfate aerosol that was tested by the nano-SMPS and the NMASS (Fig. 10). The SMPS size distribution, inverted using the same Markowsky-Twomey algorithm that is also applied to the NMASS data, displays a FWHM of 13.6% and 12.6% for the 20 and 30 nm sizes selected, respectively. Thus the Markowsky-Twomey inversion applied to the nano-SMPS slightly broadens the aerosol generated by the custom-built DMA. This is not unexpected because the inversion applies a smoothing step, as discussed in Section 4.1.

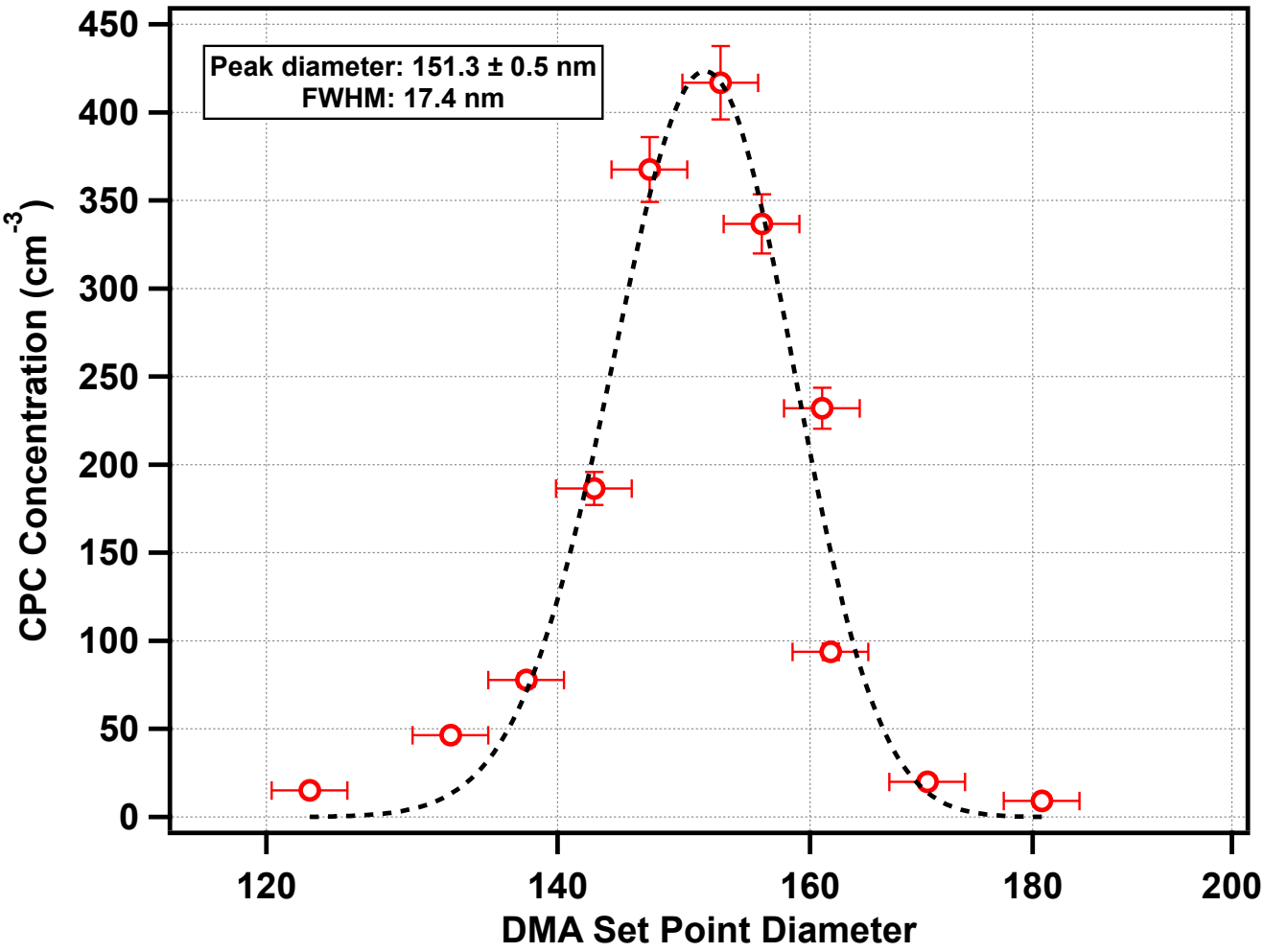

Fig. S3 Concentration of particles produced by atomizing nearly monodisperse particles, classifying them in a custom-built DMA, and counting them with a CPC.

References

Baron, P. A., and Willeke, K.: Aerosol measurement : principles, techniques, and applications, 2nd ed., Wiley, New York, xxiii, 1131 p. pp., 2001.

The Dow Chemical Company: Butanol Technical Data Sheet. 2012.

3M Electronics: Safe Sustainable Cooling Performance, Dielectric heat transfer solutions for the electronics industry, Electronics Markets, Materials Division, 3M Electronics, St Paul, MN 55144-1000, St Paul, MN, 2009.

Hinds, W. C.: Aerosol technology : properties, behavior, and measurement of airborne particles, 2nd ed., Wiley, New York, xx, 483 p. pp., 1999.

E.O. Knutson, E. O., and Whitby, K. T.: Aerosol classification by electric mobility: apparatus, theory, and applications, J. Aerosol Sci., 6, 443-451, doi:10.1016/0021-8502(75)90060-9, 1975.

The National Center for Biotechnology Information, N. C. f. B.: PubChem Compound Database; CID=263, PubChem Compound Database,

Lee, J. K., Rubow, K. L., Pui, D. Y. H., and Liu, B. Y. H.: Design and Performance Evaluation of a Pressure-Reducing Device for Aerosol Sampling from High-Purity Gases, Aerosol Sci. Technol., 19, 215-226, Doi 10.1080/02786829308959631, 1993.

Macdonald, F., and Lide, D. R.: CRC handbook of chemistry and physics: From paper to web, Abstr Pap Am Chem S, 225, U552-U552, 2003.

Materials, M. P.: Fluorinert TM Electronic Liquid FC-43 Product Information. 98-0212-2306-4 (HB), Performance Materials, 3M Center, St Paul, MN 55144-1000, St Paul, MN, 2000.

MEGlobal: Diethylene Glycol Product Guide. Dubai, UAE, 2005.

Yaws, C. L.: Thermophysical Properties of Chemicals and Hydrocarbons, Thermophysical Properties of Chemicals and Hydrocarbons, 1-809, 2008.